Journal of Applied Electrochemistry **29**: 473–480, 1999.

Electrochemical behaviour of Al, Al–Sn, Al–Zn and Al–Zn–Sn alloys in chloride solutions containing indium ions

H. A. EL SHAYEB, F. M. ABD EL WAHAB and S. ZEIN EL ABEDIN
Electrochemistry and Corrosion Laboratory, National Research Centre, Dokki, Cairo, Egypt

Received 20 July 1998; accepted in revised form 11 November 1998

Key words: activation, aluminium alloys, chloride, indium, tin, zinc

Abstract

The electrochemical behaviour of pure aluminium and three of its alloys were investigated in 0.6 M NaCl in the presence and absence of In^{3+} ions. The study comprised polarization and potentiostatic current–time measurements complemented by SEM–EDAX investigation. In 0.6 M NaCl the corrosion resistance of the alloys decreases in the following order: Al < Al–Sn < Al–Zn ≃ Al–Zn–Sn. The addition of In^{3+} ions to the test electrolyte revealed activation of pure Al which increases with increase of In^{3+} concentration. Similar results were obtained for the binary Al–Zn and the ternary Al–Zn–Sn alloys, while Al–Zn alloy displayed a higher activation effect with In^{3+}. It is also concluded that the existence of Zn either as an alloying element or present as a cation in the electrolyte leads to an enhanced activity of aluminium in presence of In^{3+} ions. Deactivation is observed in the case of Al–Sn alloy on addition of In^{3+} because tin retards the diffusion pathway of In to the bulk alloy, in addition to the presence of iron as an impurity in the alloy.

1. Introduction

Electrochemical studies of aluminium alloys have been mainly motivated by the application of these alloys in Al-battery and as anode materials in cathodic protection systems. Pure aluminium is oxidized rapidly by air to form an insulating film which leads to the passive behaviour of the metal in aqueous solutions [1, 2]. Therefore, unalloyed aluminium is electrochemically too passive for employment as an anode material in batteries or as a sacrificial anode in cathodic protection of steel in sea water. Elements such as indium [3–7], gallium [8–10], zinc [11, 12] and tin [13–16] have been added as alloying components for this purpose. Alternatively, activation of aluminium can be also achieved by the addition of small quantities of suitable metal salts to the electrolyte [17–25]. Numerous investigations [11–16] dealt with the corrosion behaviour of some Al alloys in which aluminium is electrochemically active. Two main explanations have been provided to account for the activation of aluminium; the first involves dissolution of the activator elements from the alloy and their subsequent redeposition on the surface [11]. This process is proposed to remove the passive film on the Al surface and, thus, causes activation. The second approach is based on the semiconducting property of the passive film. Application of the semiconducting concept is limited only to the Sn activator [26, 27]. Keir et al. [26] attributed the activation effect to the doping of the oxide film by Sn^{4+}, resulting in generation of cationic vacancies in Al_2O_3 and leading to activation of Al.

The objective of the present work is to study the electrochemical behaviour of Al, Al–Sn, Al–Zn and Al–Zn–Sn alloys in chloride solutions free and containing In^{3+} ions using electrochemical and surface analytical techniques. The study is also aimed to demonstrate the synergistic effect of zinc and indium in the activation process.

2. Experimental details

Measurements were made on ultrapure Al (99.999%), Al–Sn, Al–Zn and Al–Zn–Sn alloys, the composition of the alloys is given in Table 1. All alloys were prepared from aluminium of purity 99.61%, with high purity tin and zinc as alloying additions and were used in the cast state. The electrodes were abraded successively with

Table 1. Chemical composition of the alloys

Alloy	Fe	Si	Cu	Mn	Mg	Pb	Zn	Sn	Al
Al–Sn	0.402	0.067	0.062	0.005	0.011	0.009	0.0009	0.745	rest
Al–Zn	0.155	0.041	0.005	0.126	0.0005	0.003	4.92	0.0007	rest
Al–Zn–Sn	0.194	0.043	0.189	0.002	0.0005	0.004	5.59	0.685	rest

metallographic emery paper of increasing fineness up to 800, then degreased with acetone and washed with running distilled water. The electrodes were cathodically polarized at −1900 mV vs SCE for 3 min in the electrolyte (0.6 M NaCl) before polarization and potentiostatic current–time measurements.The electrochemical cell was made of Pyrex glass fitted with a platinum auxiliary electrode, separated from the electrolyte by a sintered glass diaphragm, and a saturated calomel reference electrode (SCE). All solutions were prepared from Analar grade reagents and distilled water.

Polarization measurements were made using a potentioscan (Wenking model POS 73). The electrode potential was changed in steps of 40 mV min^{-1} towards the positive direction up to the breakdown potential. Potentiostatic current–time tests were carried out using a potentiostat-galvanostat (Amel model 2053) with an X–Y recorder (Kipp & Zonen). The treated electrodes were passivated in the electrolyte for 20 min at −1050 mV and −980 mV in the case of Al and Al–Sn alloy respectively, and at −1140 mV in the case of Al–Zn and Al–Zn–Sn alloys. Appropriate amounts of dissolved $InCl_3$ or $ZnCl_2$ salts were then added to the electrolyte maintaining the Cl^- ion concentration constant. The solution was agitated slowly by a magnetic stirrer to mix the additives with the electrolyte. A scanning electron microscope (SEM: JSM T20 of Joel Japan) and energy dispersive X-ray analyser (EDAX) were utilized to examine the electrode surface.

3. Results and discussion

3.1. *Polarization measurements*

Polarization curves of Al, Al–Sn, Al–Zn and Al–Zn–Sn alloys in 0.6 M NaCl solution are displayed in Figure 1. The polarization curve for pure aluminium is characterized by a flat passive region extends from −1600 to −780 mV vs SCE. The potential at the end of the passive region represents the breakdown potential at which the onset of pitting attack takes place. The passive current density is very low, 3 μA cm^{-2}, showing the passive behaviour of Al and revealing the stability of the passive film in this medium.

The polarization curve of Al–Sn alloy exhibits an active behaviour compared to that of pure Al. The pitting potential takes more negative value (−900 mV) than pure Al and a noticeable reduction of the passive region is recorded. This behaviour is attributed to the presence of Sn as an alloying element leading to an electrochemical activity of the alloy [26, 27] due to modification in the chemistry of the film leading to the active dissolution of Al [14]. Tin ions are known to be incorporated in the Al_2O_3 film enhancing the chloride ion migration from film–solution interface to the metal film interface [26, 27]. The outer most oxide layer on Al–Sn alloy is more hydroxy in nature than that of Al [14]. Hashimoto et al. [28] suggested that the higher hydroxide content is responsible for the poor protective nature of the films. Accordingly, the active dissolution of Al–Sn alloy resulted not only from enhancement of defects created in the oxide as a result of Sn addition [15] but also from the higher hydroxide content of the oxide film [14].

The polarization behaviour of Al–Zn and Al–Zn–Sn alloys in 0.6 M NaCl shows some differences from that of Al–Sn. The pitting potential of the two alloys shifted to more negative values than Al–Sn alloy (−1000 mV for Al–Zn and −1020 mV for Al–Zn–Sn). It is known [16, 29, 30] that the presence of Zn and/or Sn as alloying components shift the chloride ion adsorption to more negative values, hence the pitting potential moves to the negative direction. The peak observed on the anodic

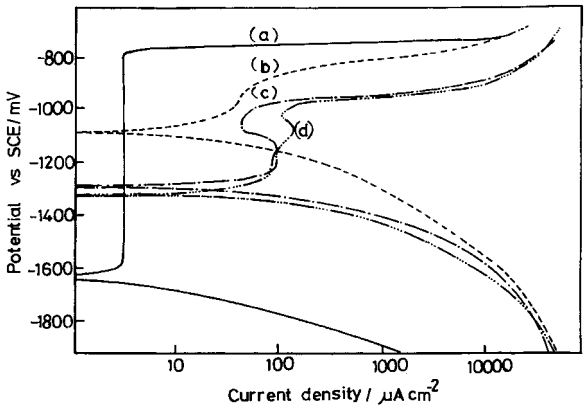

Fig. 1. Polarization curves of (a) Al, (b) Al–Sn, (c) Al–Zn and (d) Al–Zn–Sn in 0.6 M NaCl.

branch of the polarization curves of Al–Zn and Al–Zn–Sn alloys can be explained in terms of the oxidation of elemental zinc to $Zn(OH)_2$ [31]. The retardation of the $Zn(OH)_2$ peak in the case of Al–Zn–Sn alloy can be ascribed to the presence of Sn as an alloying element, which reduces the oxidation process of zinc for the increase in the active dissolution of the alloy.

The effect of adding different concentrations of In^{3+} on the polarization behaviour of Al and the tested alloys in 0.6 M NaCl solution was investigated, Figure 2. As shown in Figure 2(a), the pitting potential of the Al electrode moves towards more negative values and a reduction of the passive region takes place with increase in In^{3+}concentration. The reduction step observed on the cathodic branch of the polarization curve at relatively higher concentration of In^{3+} is due to the deposition of indium at the surface.

On the one hand, additions of In^{3+} to the electrolyte causes an insignificant shift in the pitting potential of the binary Al–Sn electrode in the negative direction, Figure 2(b). At $C \geqslant 10^{-2}$ M In^{3+}, a reduction step for the deposition of In is observed in the cathodic branch of the polarization curve as in the case of Al . On the other hand, In^{3+} causes a pronounced influence, leading to further activation of Al–Zn and Al–Zn–Sn alloys, Figure 2(c) and (d). The pitting potential of the Al–Zn electrode shifts in the negative direction with increase in In^{3+}concentration, Figure 2(c). The oxidation peak of $Zn/Zn(OH)_2$ is affected by increase in In^{3+} concentration which may be attributed to the greater amount of the deposited In which covers the Zn atom on the surface. In the case of Al–Zn–Sn alloy, the pitting potential shifts in the negative direction at In^{3+} concentrations greater than 10^{-3} M.

3.2. *Current–time measurements*

3.2.1. *Effect of In^{3+} addition*

The potentiostatic current–time measurements give further valuable information about the effect of In^{3+} addition on the activation of Al and further activation of Al–Sn, Al–Zn and Al–Zn–Sn alloys. Figure 3 presents the current–time decay profiles of pure aluminium polarized at −1050 mV (which is in the passive range) in 0.6 M NaCl solution to which a definite amount of In^{3+} was added after 20 min. The curves exhibit a rapid decrease in the anodic current in the early minutes of passivation then become constant, indicating passive film formation. The addition of In^{3+} to the solution after 20 min causes no immediate effect and the

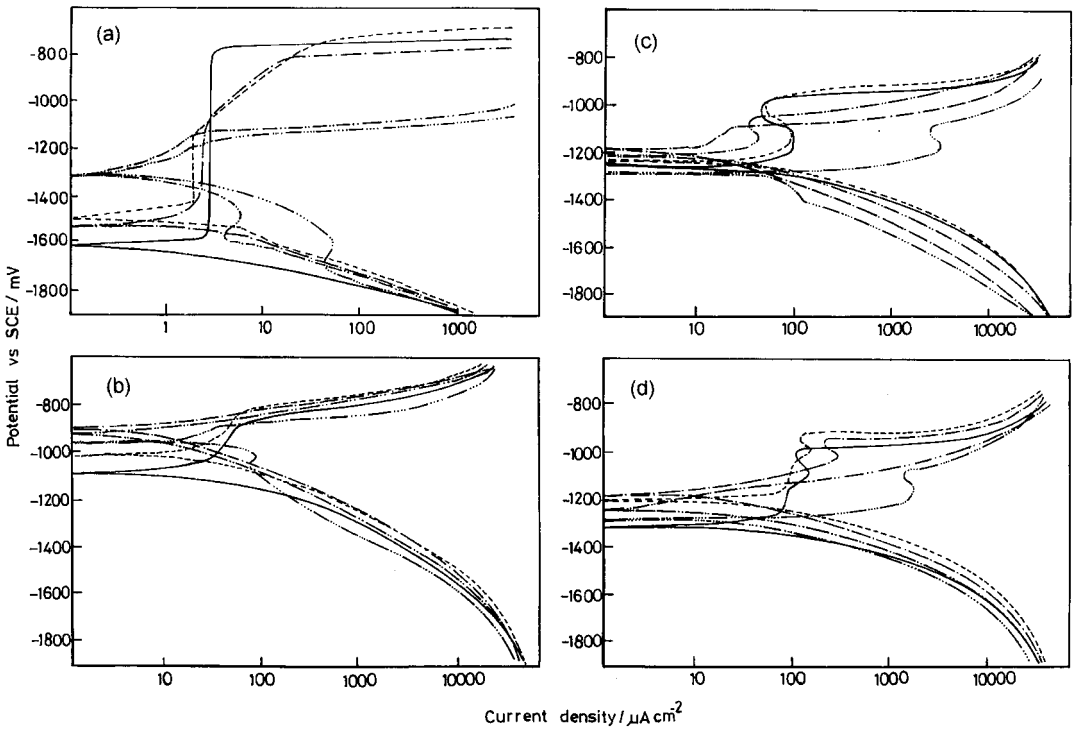

Fig. 2. Polarization curves of (a) Al, (b) Al–Sn, (c) Al–Zn and (d) Al–Zn–Sn in 0.6 M NaCl and different concentrations of In^{3+}. Curves (—) without In^{3+}, (- - -) 10^{-4} M In^{3+}, (–·–) 10^{-3} M In^{3+}, (–··–) 3×10^{-3} M In^{3+} and (–· · ·–) 10^{-2} M In^{3+}, for Al, Al–Sn and Al–Zn–Sn. Curves (—) without In^{3+}, (- - - -) 10^{-4} M In^{3+}, (–··–) 5×10^{-4} M In^{3+}, (–·–) 10^{-3} M In^{3+} and (–· · ·–) 10^{-2} M In^{3+} for Al–Zn.

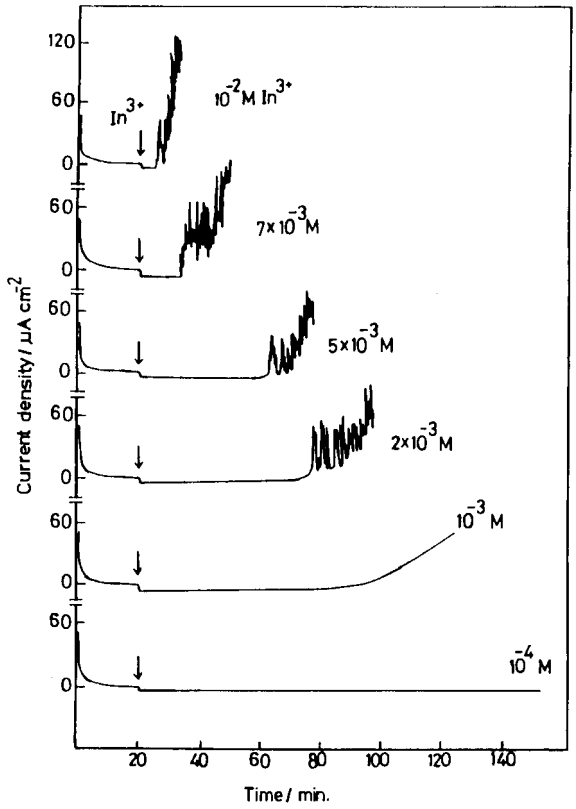

Fig. 3. Current–time curves of Al electrode passivated at −1050 mV in 0.6 M NaCl solution to which different concentrations of In^{3+} were added after 20 min.

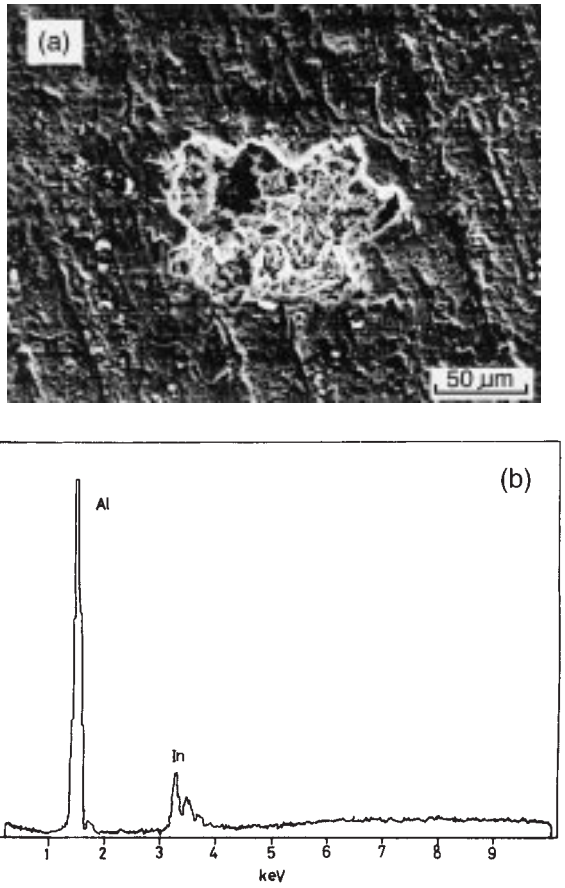

Fig. 4. (a) SEM micrograph of Al surface obtained after potentiostatic polarization at −1050 mV in 0.6 M NaCl + 5×10^{-3} M In^{3+}. (b) EDAX analysis inside the pit shown in the micrograph.

current remains constant for a certain time which is the induction period before activation. After the induction period, the anodic current increases with fluctuations, indicating the start of passivity breakdown. As a consequence of In^{3+} addition, activation takes place at different rates, increasing with increase in In^{3+} concentration. SEM–EDAX examination of the electrode surface, Figure 4, shows that the attack is localized. The scanning electron micrograph, Figure 4(a), shows the surface morphology of an Al electrode after passivity breakdown under potentiostatic conditions in 0.6 M NaCl containing 5×10^{-3} M In^{3+}. The surface exhibits crystallographic pitting attack with a high indium concentration, as detected by the corresponding EDAX analysis, Figure 4(b).

The curves of Figure 5 display the current–time measurements of Al–Sn alloy polarized in 0.6 M NaCl at −980 mV for 20 min, followed by addition of a definite amount of In^{3+}. The curves exhibit a rapid decrease in the anodic current in the early moments of immersion. Before In^{3+} ion addition the current attains an almost constant value with fluctuations indicating incomplete passivation of the electrode. On addition of

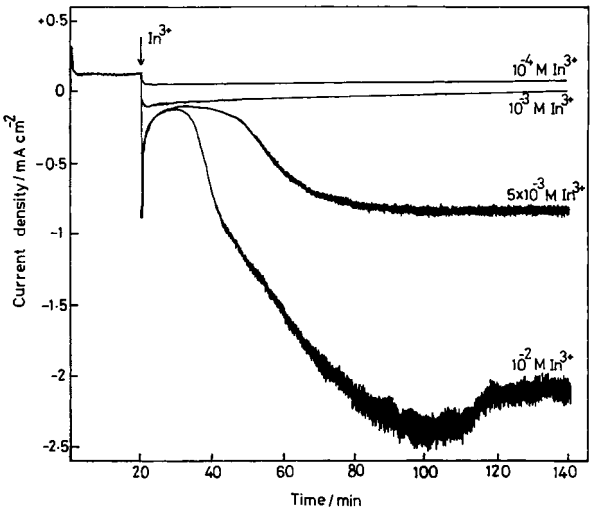

Fig. 5. Current–time curves of Al–Sn electrode passivated at −980 mV in 0.6 M NaCl solution to which different concentrations of In^{3+} were added after 20 min.

lower concentrations of In^{3+}, the cathodic current increases and remains constant throughout the experiment. At higher concentrations ($C \geqslant 5 \times 10^{-3}$ M In^{3+}), the cathodic current increases and remains almost constant for a definite time, depending on In^{3+} concentration. A further increase in the cathodic current is then recorded up to a constant value. This is due to the increased amount of deposited indium. This fact is confirmed by SEM–EDAX examination of the surface of the Al–Sn electrode passivated at −980 mV in 0.6 M NaCl and 5×10^{-3} M In^{3+}, Figure 6. The deposition of a large amount of indium is clearly seen from the micrograph in Figure 6(a), where the deposit is analysed as indium by the corresponding EDAX profile, Figure 6(b).

Unlike the behaviour of Al–Sn alloy, Al–Zn alloy displays a completely different behaviour on addition of In^{3+} to the electrolyte during potentiostatic I/t measurements ($E = -1140$ mV), Figure 7. The anodic current decreases rapidly in the early stages, then takes an approximate constant value. Addition of In^{3+}, after 20 min, causes a noticeable activating effect. The concentration of 10^{-4}M In^{3+} is too low to activate the electrode and the current is unchanged during the time of the experiment. This is attributed to insufficient deposited In to promote activation. At concentrations more than 10^{-4} M and less than 3×10^{-3} M, the anodic current increases after an induction period, indicating the starting of passivity breakdown. The induction period decreases with increase in In^{3+} concentration until it disappears at $C \geqslant 3 \times 10^{-3}$ M and the anodic current increases rapidly, with fluctuations, indicating accelerated activation. The large fluctuations observed in the I/t curve at a concentration of 10^{-2} M In^{3+} can be attributed to an activation–repassivation process resulting from the accelerated deposition of In. Surface examination of the Al–Zn electrode by SEM, Figure 8(a), after activation by 10^{-3} M In^{3+} during potentiostatic I/t measurements at −1140 mV in 0.6 M NaCl showed localized attack with typical pits containing indium as detected by EDAX, Figure 8(b).

Figure 9 displays current–time curves of the ternary Al–Zn–Sn alloy under the same experimental conditions. There is a resemblance between these curves and those for the Al–Zn alloy. However, higher concentrations of In^{3+} are required to achieve a comparable degree of activation. It seems that the presence of Sn in the alloy suppresses the activation process by In^{3+}, as seen earlier in the case of Al–Sn alloy (*cf.* Figure 5). These results are in agreement with those obtained from the polarization measurements. The SEM micrograph in Figure 10(a) shows a corroded surface of Al–Zn–Sn alloy after activation by 10^{-3} M In^{3+}. The localized

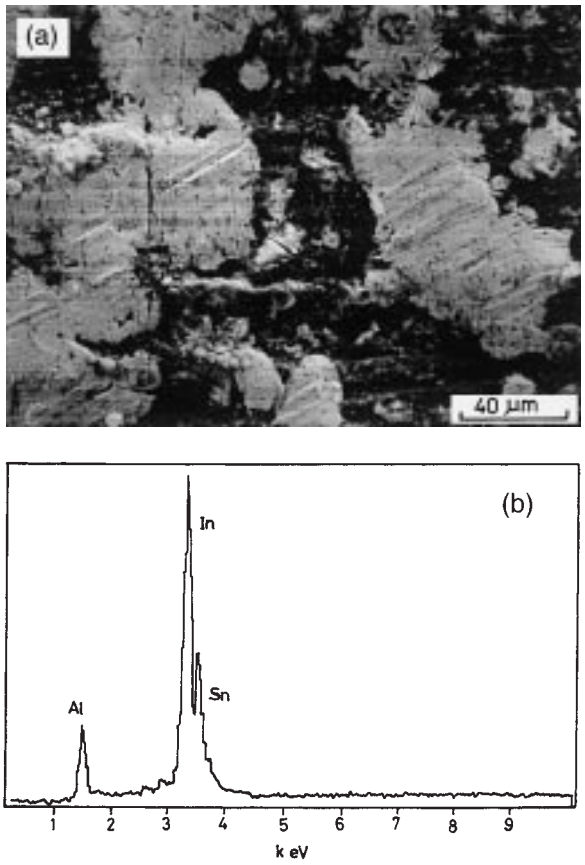

Fig. 6. (a) SEM micrograph of Al–Sn electrode obtained after potentiostatic polarization at –980 mV in 0.6 M NaCl + 5×10^{-3} M In^{3+}. (b) EDAX analysis of the area shown in the micrograph.

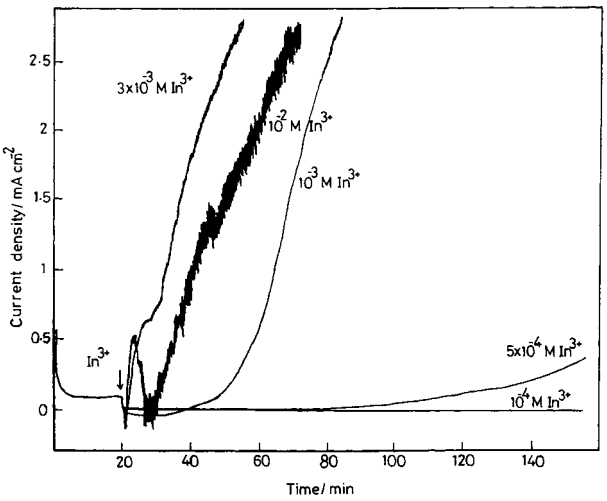

Fig. 7. Current–time curves of Al–Zn electrode passivated at –1140 mV in 0.6 M NaCl solution to which different concentrations of In^{3+} were added after 20 min.

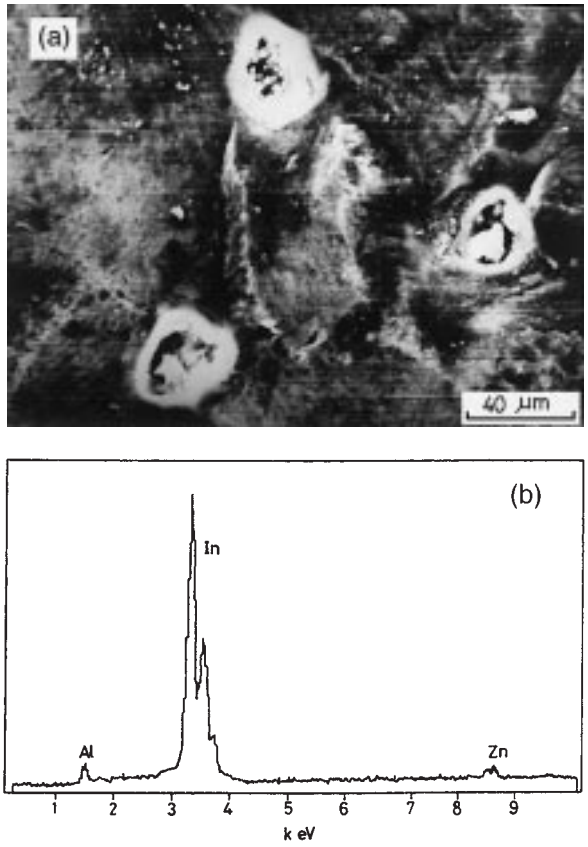

Fig. 8. (a) SEM micrograph of Al–Zn electrode obtained after potentiostatic polarization at –114 mV in 0.6 M NaCl + 10^{-3} M In^{3+}. (b) EDAX analysis inside the pit shown in the micrograph.

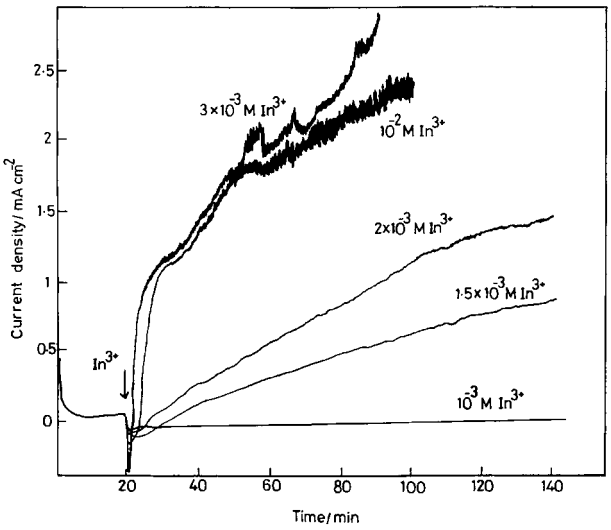

Fig. 9. Current–time curves of Al–Zn–Sn electrode passivated at −1140 mV in 0.6 M NaCl solution to which different concentrations of In^{3+} were added after 20 min.

attack is characterized by broad shallow cavities containing indium, Figure 10(b).

In the light of the above results, the alloying components have an important role in the activation or deactivation processes by indium ions. However, the deactivation observed on addition of In^{3+}, for Al–Sn alloy, can be attributed to the presence of Fe (0.402%) as an impurity in the alloy. The existence of Sn also retards the diffusion path of the activator ion to the bulk of the alloy matrix. The activation process takes place only if the activator ions (In^{3+}) are incorporated in the outermost surface layer of aluminium [3, 18, 20, 32]. On the other hand, the activating effect of In^{3+} on Al–Zn alloy is higher than its effect on pure Al. This is ascribed to the presence of Zn as an alloying component in the alloy. Breslin et al. [33, 34] suggested that the presence of zinc, either as an alloying element or as cations in the electrolyte, promotes the nucleation of $ZnAl_2O_4$ spinel which gives rise to increased defects and cracking of the protective layer. Once the indium is deposited, at the newly generated defects, it may diffuse into the bulk

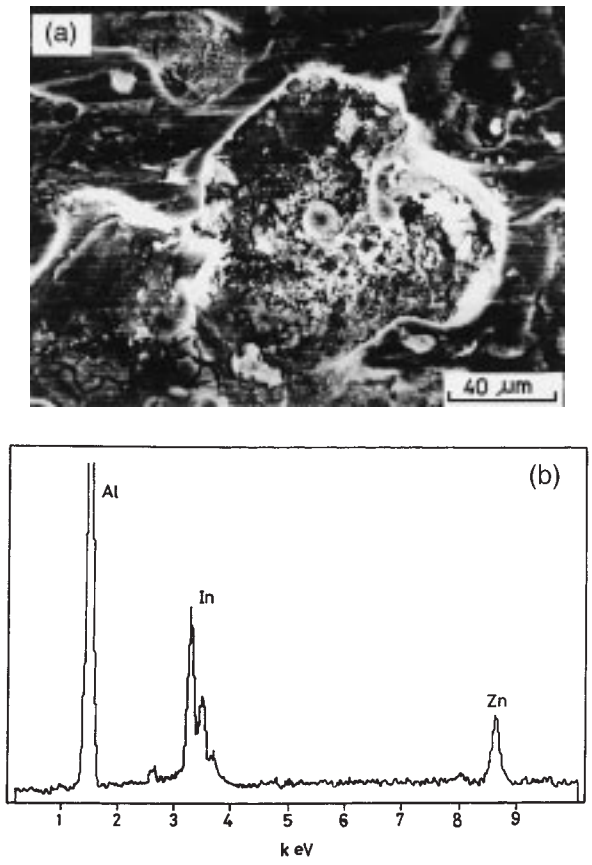

Fig. 10. (a) SEM micrograph of Al–Zn–Sn electrode obtained after potentiostatic polarization at –1140 mV in 0.6 M NaCl + 10^{-3} M In^{3+}. (b) EDAX analysis inside the cavity shown in the micrograph.

material owing to its high mobility, enabling true In/Al contact and facilitating the adsorption of chloride ions at the surface (i.e., activation) due to its greater affinity to indium [35]. In the case of Al–Zn–Sn alloy, the zinc plays the same role, as before, and accelerated deposition of In occurs at the defect centers. However, the presence of Sn retards, to some extent, the diffusion of In to the bulk alloy. Accordingly, the activating effect of In^{3+} is reduced for Al–Zn–Sn compared to Al–Zn alloy. The mechanisms of film breakdown of pure Al, Al–Zn and Al–Zn–Sn alloys are similar. The initiation step depends on both the availability of defect centres and on the deposition of In at such centres, which is responsible for the adsorption of Cl^- at more negative potentials [36].

3.2.2. *Effect of In^{3+} and Zn^{2+} addition*

It seemed of interest to examine the effect of Zn^{2+} ion on the activation of pure Al by In^{3+} ion to clarify the interrelationship between indium and zinc. Figure 11 shows the effect of Zn^{2+} ion alone and with In^{3+} ion on the activation of pure Al in 0.6 M NaCl during potentiostatic current–time measurements at −1050 mV. It is clear that zinc ion alone of 10^{-2} M concentration has no influence on the Al electrode but the presence of both Zn^{2+} and In^{3+} in the electrolyte increases the activation process, as indicated from the shorter induction period compared to that obtained in the case of In^{3+} alone. The extent of activation increases with increase in Zn^{2+} content at a constant In^{3+} concentration (5×10^{-3} M). It is interesting to note that the increase in current accompanied by fluctuations in the case of In^{3+} alone indicates activation–repassivation. On the other hand, when adding Zn^{2+} together with In^{3+} the anodic current increases abruptly without fluctuations. Although, aluminium can be activated with zinc as an alloying component [37, 38], no activation is observed on adding Zn^{2+} ion, Figure 11. This can be attributed to the tendency of zinc to dissolve from the surface after deposition, combined with its much lower mobility into the bulk metal. Moreover, aluminium should be protected cathodically at the expense of the deposited zinc and, consequently, dissolution of zinc takes place from the surface. When In^{3+} and Zn^{2+} are present, accelerated deposition of In occurs, since adsorption of Zn^{2+} on the electrode surface mainly takes place, thus permitting preferred In deposition on the freshly nucleated Zn where In deposition is easier on Zn than on Al [17]. This situation is verified by

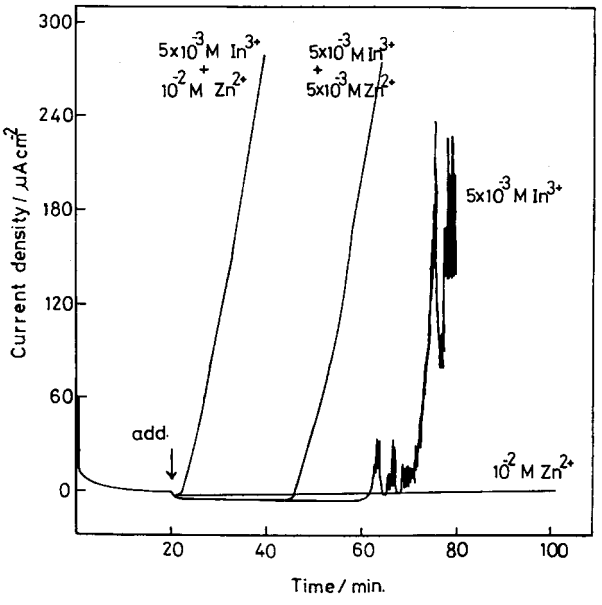

Fig. 11. Current–time curves of Al electrode passivated at –1050 mV in 0.6 M NaCl solution to which Zn^{2+} and/or In^{3+} were added after 20 min. (a) 10^{-2} M Zn^{2+}, (b) 5×10^{-3} M In^{3+}, (c) 5×10^{-3} M In^{3+} + 5×10^{-3} M Zn^{2+} and (d) 5×10^{-3} M In^{3+} + 10^{-2} M Zn^{2+}.

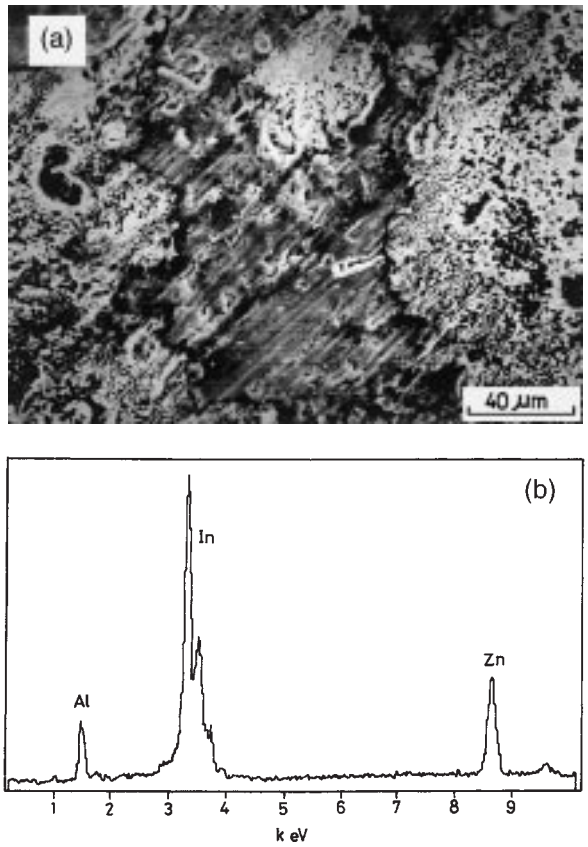

Fig. 12. (a) SEM micrograph of Al electrode obtained after potentiostatic polarization at –1050 mV in 0.6 M NaCl + 5×10^{-3} M In^{3+} + 10^{-2} M Zn^{2+}. (b) EDAX analysis of the area shown in the micrograph.

SEM–EDAX examination of Al passivated at −1050 mV in 0.6 M NaCl to which 5×10^{-3} M In^{3+} and 10^{-2} M Zn^{2+} were added after 20 min, Figure 12. The micrograph, Figure 12(a), shows the severity of attack due to the deposition of large amounts of In and Zn, as detected by EDAX profile, Figure 12(b). As a consequence of Zn deposition, sufficient nucleation of $ZnAl_2O_4$ spinel occurs and causes rupture of the protective oxide film enabling In^{3+} to play its role in the activation process. The recorded enhanced activity of aluminium in the presence of Zn^{2+} and In^{3+} agrees with other investigations [11, 34, 39].

4. Conclusion

The following statements can now be made:

(i) The pitting potential of the tested alloys in 0.6 M NaCl increases in the negative direction in the order Al < Al–Sn < Al–Zn ≃ Al–Zn–Sn.

(ii) The addition of In^{3+} ion produced activation of pure Al, Al–Zn, and Al–Zn–Sn electrodes and the extent of activation increases with increase in In^{3+} concentration.

(iii) The activating effect of In^{3+} on Al–Zn alloy is higher than its effect on pure Al due to the presence of Zn, which promotes nucleation of $ZnAl_2O_4$ spinel which, in turn, gives rise to increased defects in the protective layer.

(iv) The activating effect of In^{3+} is reduced for Al–Zn–Sn alloy compared to that of Al–Zn alloy.

(v) Deactivation is observed in the case of Al–Sn alloy on addition of In^{3+} due to the presence of Sn which retards the diffusion pathway of In to the bulk of the alloy, in addition to the presence of iron as an impurity.

(vi) The existence of Zn, either as an alloying element or as a cation in the electrolyte, leads to enhanced activity of aluminium in the presence of In^{3+} ions

(vii) The mechanisms of activation of pure Al, Al–Zn and Al–Zn–Sn are similar. The initiation step depends on both the availability of defect centres and on the deposition of In at such centres.

References

1. P.A. Malachesky, *in* '*Encyclopedia of Electrochemistry of the Elements*', vol. 6, edited by A.J. Bard (Marcel Dekker, NewYork, 1976), p. 63.
2. S. Real, M. Urquidi-Macdonald and D.D.Macdonald, *J. Electrochem. Soc.* **135** (1988) 1633 and 2397.
3. S.B. Saidman, S.G. Garcia and J.B. Bessone, *J. Appl. Electrochem.* **25** (1995) 252.
4. C.B. Breslin and W.M. Carroll, *Corros. Sci.* **34** (1993) 1099.
5. C.B. Breslin and W.M. Carroll, *Corros. Sci.* **36** (1994) 85.
6. L. Bai and B.E. Conway, *J. Appl. Electrochem.* **22** (1992) 131.
7. A. Venugopal and V.S. Raja, *Br. Corros. J.* **31** (1996) 318.
8. C.B. Breslin and W.M. Carroll, *Corros.Sci.* **33** (1992) 1735.
9. C.D.S. Tuck, J.A. Hunter and G.M. Scamans, *J. Electrochem. Soc.* **134** (1987) 2070.
10. A.R. Despić, D.M. Drazić, M.M. Purenović and N. Ciković, *J. Appl. Electrochem.* **6** (1976) 527.
11. M.C. Reboul, P.H. Gimenez and J.J. Rameau, *Corrosion.* **40** (1984) 366.
12. A. Tamada and Y. Tamura, *Corros. Sci.* **34** (1993) 261.
13. M. Kliskić, J. Radosević and L.J. Aljinović, *J. Appl. Electrochem.* **24** (1994) 814.
14. A. Venugopal, P. Veluchamy, P. Selvam, H. Minoura and V.S. Raja, *Corrosion* **53** (1997) 808.
15. T. Valand and G. Nilsson, *Corros. Sci.* **17** (1977) 931.
16. D.R. Salinas and J.B. Bessone, *Corrosion* **47** (1991) 665.
17. S.B. Saidman and J.B. Bessone, *J. Appl. Electrochem.* **27** (1997) 731.
18. S.B. Saidman and J.B. Bessone, *Electrochim. Acta* **42** (1997) 413.
19. F. Holzer, S. Müller, J. Desilvestro and O. Haas, *J. Appl. Electrochem.* **23** (1993) 125.
20. G. Burri, W. Luedi and O. Haas, *J. Electrochem. Soc.* **136** (1989) 2167.
21. J.U. Chavarin, *Corrosion* **47** (1991) 472.
22. W.M. Carroll and C.B. Breslin, *Br. Corros. J.* **26** (1991) 255.
23. A.H. Al-Saffar, V. Ashworth, W.A. Grant and R.P.M. Procter, *Corros. Sci.* **18**(1978) 687.
24. J.E. Equey, S. Müller, A.T. Sukada and O. Haas, *J. Appl. Electrochem.* **19** (1989) 65.
25. A. Venugopal and V.S. Raja, *Corros. Sci.* **39** (1997) 1285.
26. D.S. Keir, M.J. Pryor, P.R. Sperry, *J. Electrochem. Soc.* **114** (1967) 777.
27. D.S. Keir, M.J. Pryor, P.R. Sperry, *J. Electrochem. Soc.* **116** (1969) 319.
28. K. Hashimoto and K. Asami, *Corros. Sci.* **19** (1979) 251.
29. J.T. Reading and J.J. Newport, *Mater. Protect.* **5** (1966) 15.
30. J.B. Bessone, R.A. Suarez Baldo and S.M.de De Micheli, *Corrosion* **37** (1981) 533.
31. A.M. Shams El-Din, F.M. Abd El Wahab and S.M. Abd El Haleem, *Werkst. Korros.* **5** (1973) 389.
32. C.B. Breslin, L.P. Friery and W.M. Carroll, *Corrosion* **49** (1993) 895.
33. C.B. Breslin, L.P. Friery and W.M. Carroll, *Corros. Sci.* **36** (1994) 85.
34. C.B. Breslin, L.P. Friery, *Corros. Sci.* **36** (1994) 231.
35. F.A. Cotton and G. Wilkinson, '*Advanced Inorganic Chemistry*', 4th edn (J. Wiley & Sons, New York), 1980, p. 334.
36. H.A. El Shayeb, F.M. Abd El Wahab, S. Zein El Abedin, submitted to *J. Appl. Electrochem.*
37. I.L. Muller and J.R. Galvele, *Corros. Sci.* **17** (1977) 995.
38. P.M. Natishan, E. McCafferty and G.K. Hubler, *J. Electrochem. Soc.* **133** (1986) 1061.
39. A. Venugopal and V.S. Raja, *Corros. Sci.* **39** (1997) 2053.